Supporting Information

Time-resolved insight into the photosensitized generation of singlet oxygen in endoperoxides

Lara Martínez-Fernández,[a] Jesús González-Vázquez*[a], Leticia González[b], and Inés Corral*[a]

[a]Universidad Autónoma de Madrid, Departamento de Química, 28049 Cantoblanco, Madrid, Spain. E-mail: ines.corral@uam.es, jesus.gonzalezv@uam.es

[b]Institute of Theoretical Chemistry, University of Vienna, Währingerstrasse 17, 1090 Vienna, Austria

Computational details

The active space used in this work (except otherwise specified) contains 14 electrons in 12 orbitals, and involves 2 pairs of π_{CC}/π^*_{CC}, π_{OO}/π^*_{OO}, and the σ orbitals sitting on the oxygen atoms $\sigma_{CO}/\sigma^*_{CO}$ (2pairs) and $\sigma_{OO}/\sigma^*_{OO}$, see Figure S1. The CASSCF/ANO-S level of theory was used for the optimization of the stationary points with the required number of roots in each case. Final energies at these geometries were calculated at MS-CASPT2//CASSCF/ANO-RCC level of theory considering 4 singlet and 4 triplet states.

Additional Computational details for the location of the TS.

For the location of the transition state (TS_{O2}) a combination of different techniques was employed. First, a relax scan along the stretching of the C-O distance was performed with the (14,12) active space (see Fig. S1) combined with the 6-31G* basis set. The starting geometry was the one of the Min_{SW} and the CO distance was increased in regular steps of 0.05 Å. Then, due to the sharp topology of the potential energy surface around this TS a constrained optimization fixing the CO distance to the value 1.9 Å was necessary. Finally, minimum energy paths from the TS structure were performed to ensure its connection with Min_{SW} and Min_{O2}, see Figure S2 and S3.

Minimum Energy Paths (MEP)

Minimum Energy paths were computed at CASSCF/6-31G* to connect stationary points (Figure S3 and S4) and from the Franck-Condon (FC) region following the first and second excited state (Figure S5A). When these MEPs reach degeneracy regions the calculation was continued following the root of in each case.

Dynamic Study

CASSCF was found to significantly overestimate the excitation energies at the FC region providing a shifted absorption spectrum taking CASPT2 as a reference. For the ground state, the obtained CASSCF and CASPT2 profiles are very similar and in *quantitative* agreement whereas for the excited states CASSCF and CASPT2 profiles are only in *qualitative* agreement. Since the CASSCF and CASPT2 energy gap between excited and ground state potentials along the MEPs of interest (and therefore the excited

state gradients) were found to differ in average by a factor of 0.75, this factor was used to scale all the gradients and energies in the dynamical simulations. This scaling was however suppressed whenever the system reaches the first singlet potential, where the CASSCF and CASPT2 profiles become similar.

Figure S6 and S7 show the simulated absorption spectra of CHDEPO calculated at CASSCF and CASPT2 levels of theory, respectively, superimposed to the different contributions of the singlet excited states. Figure S8 depicts the time evolution of the representative trajectory resulting in benzoquinone and H_2 whose snapshots are plotted in Figure 7B of the main paper.

SHARC scheme

The movement of the electrons and nuclei are treated in different frameworks: the nuclei are considered as classical particles are followed using Newton's equations integrated with the velocity Verlet algorithm[1] with a time step Δt whereas the electronic part is simulated propagating the time dependent Schrödinger equation (TDSE) expanding the wavefunction in eigenfunctions, $\psi_i[r; R(t)]$, generated for a given nuclear geometry with the form:

$$\Psi(r, R, t) = \sum_i c_i(t)\psi_i[r; R(t)] \tag{1}$$

where r and R are collective coordinates representing the electronic and nuclear coordinates, respectively. Introducing this wavefunction in the TDSE and integrating over r we obtain:

$$\frac{\partial c_j(t)}{\partial t} = -\sum_i \left\{\frac{i}{\hbar} H_{ji}[R(t)] + K_{ji}[R(t)]\right\} c_i(t) \tag{2}$$

where the Hamiltonian matrix (including Spin-Orbit coupling), H_{ji}, is represented by

$$H_{ji} = \int_r \psi_j^\star \hat{H} \psi_i dr \tag{3}$$

and the non-adiabatic coupling, K_{ji}, is apporximated as the overlap of the wavefunction at two consecutive steps

$$K_{ji} = \int_r \psi_j^\star \frac{\partial}{\partial t} \psi_i dr \approx \frac{\delta_{ji} - \int_r \psi_j^\star(t)\psi_i(t - \Delta t)dr}{\Delta t} \tag{4}$$

In the SHARC scheme,[2] the surface hopping is done in the adiabatic representation where H_{ji} is diagonal. This representation is obtained by diagonalizing the spin-orbit

coupling in a set of spin-free basis. In this work, we also propagate the electronic wavefunction in that representation. However, in order to avoid artifacts due to sudden variations of the eigenfunction character (for example in case of small spin-orbit coupling or when states of different symmetry cross), the order of the eigenfunctions (and their signs) is given by minimizing the K_{ji} matrix with respect the previous nuclear geometry, maintaining the Hamiltonian diagonal. This treatment was already tested in Ref 3, in the context of laser induced phenomena.

Since the electronic part requires a smaller time step than the nuclear part ($\Delta t = 0.5$ fs), the nuclear time step was divided in 50 substeps, where the Hamiltonian matrix, H_{ji}, and the non-adiabatic couplings, K_{ji}, between time t and $t + \Delta t$ were obtained using a bicubic spline algorithm considering the last five *ab initio* results. Finally, equation (2) was solved with a 4th Runge Kutta algorithm and the probability of jumping from the state *j* to the state *i* was obtained by the Tully's Surface Hopping[4] formula:

$$P_{ji} = \frac{2\Re\left[c_j^\star c_i^\star \left(\frac{i}{\hbar} H_{ji} + K_{ji}\right)\right]}{c_j^\star c_j} \Delta t \tag{5}$$

At the end of every nuclear step, the variables are reordered according to their energy inducing diabatic hops if the actual state modifies its order.

(1) Verlet, L. *Phys. Rev.*, **1967**, 159, 98; Verlet, L. *Phys. Rev.*, **1968**, 165, 201.
(2) Richter, M; Marquetand, P; González-Vázquez, J; Sola, I; González, L. *J. Chem. Theory Comput.*, **2011**, 7, 1253
(3) Bajo, J. J.; González-Vázquez, J; Sola, I; Santamaria, J; Richter, M; Marquetand, P; González, L. *J. Phys. Chem. A*, **2012**, 116, 2800.
(4) Tully, J. C. *J. Chem. Phys*. **1990**, 93, 1061.

Figure S1. Orbitals included in the (14,12) active space optimized for the ground state equilibrium minimum of CHDEPO.

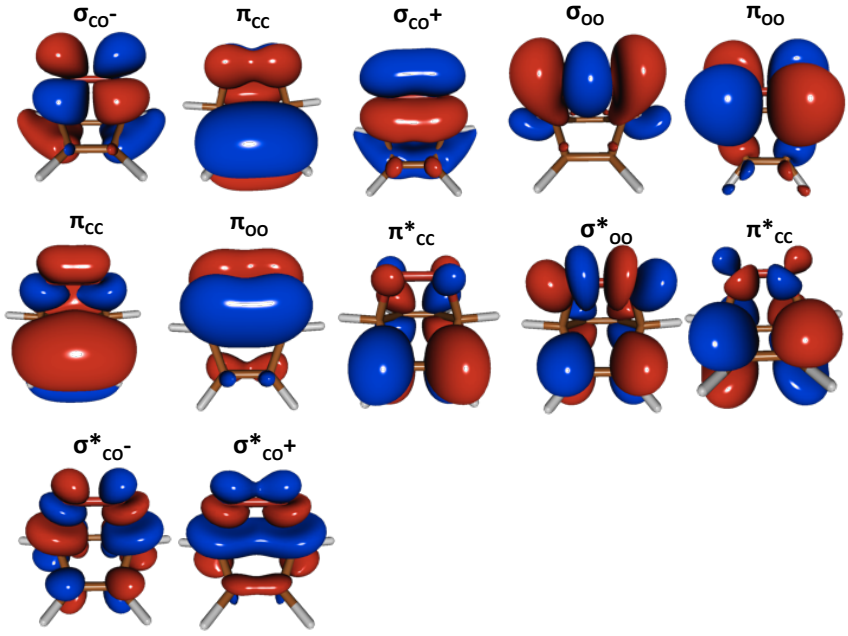

Figure S2. CASSCF relaxed scan along the stretching of the C-O distance from the optimized Min_{SW} structure. Distances in Å and energies in eV relative to Min_{O2}.

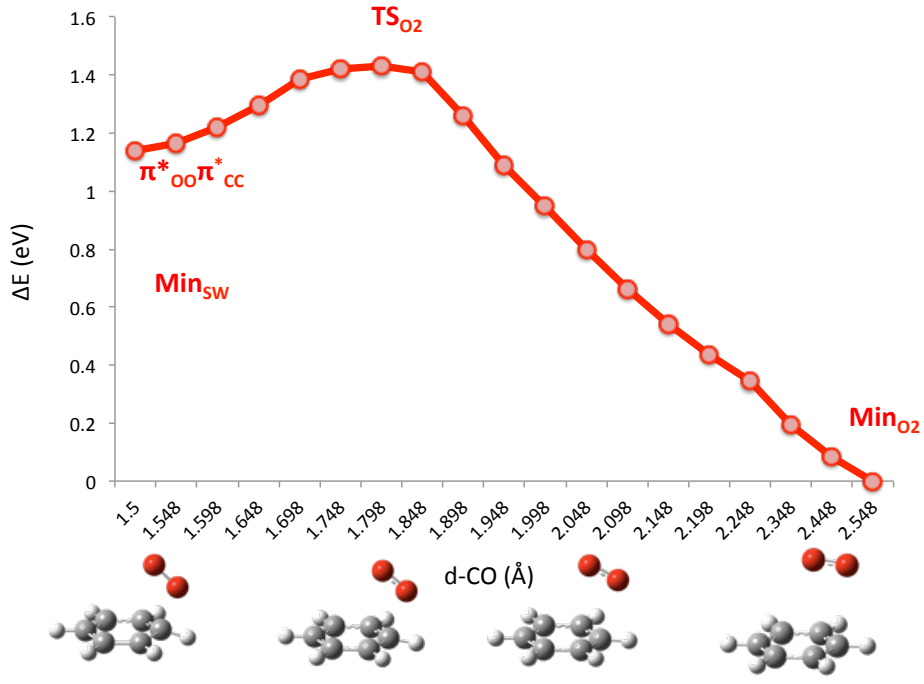

Figure S3. CASSCF Minimum energy paths from the TS_{O2} to the two falnking minima Min_{SW} and Min_{O2}. Distances in Å and energies in eV relative to Min_{O2}.

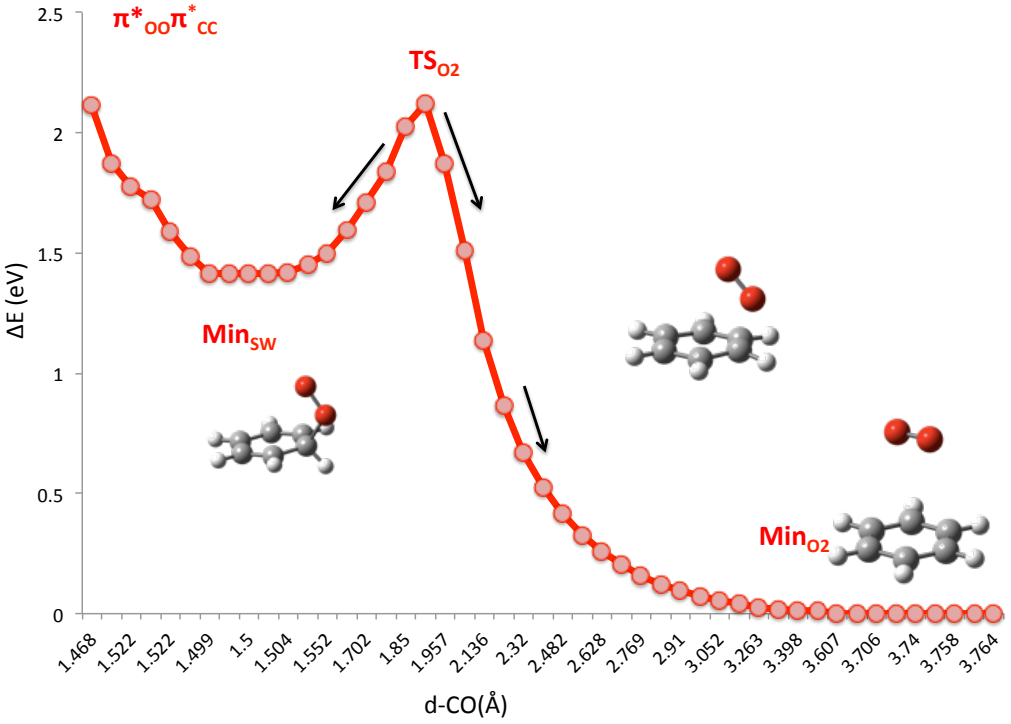

Figure S4. CASSCF Minimum energy path from the $CI_{S1/S0}$ to minima Min_{SW}. Distances in Å and energies in eV relative to Min_{SW}.

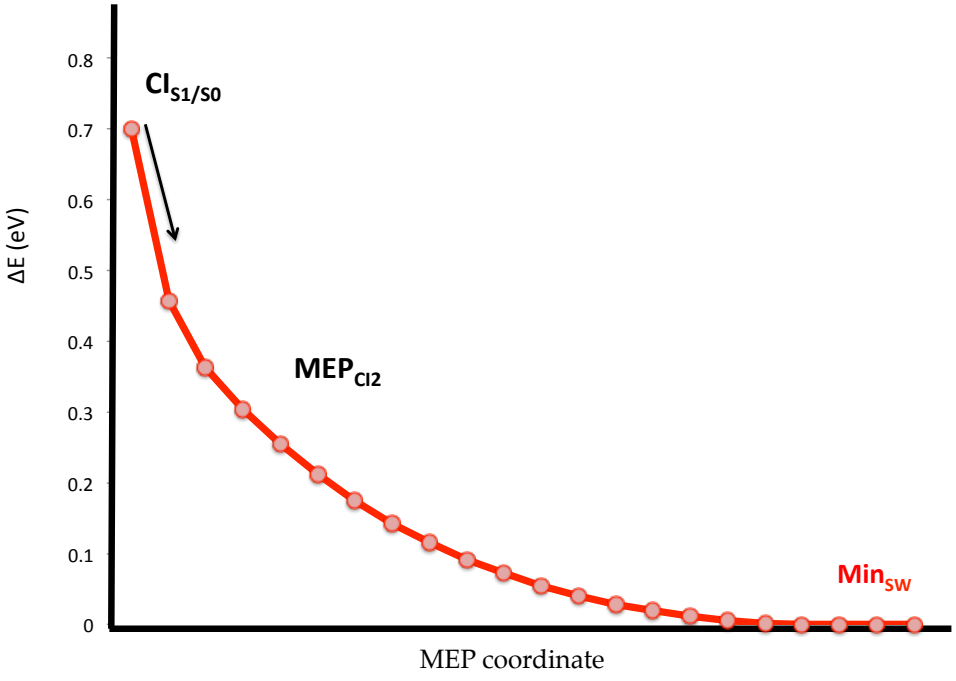

Figure S5. CASSCF Minimum energy path from the FC region (a) following the S_1 state and (b) following the S_2 state. Distances in Å and energies in eV relative to the ground state (GS) at the FC equilibrium.

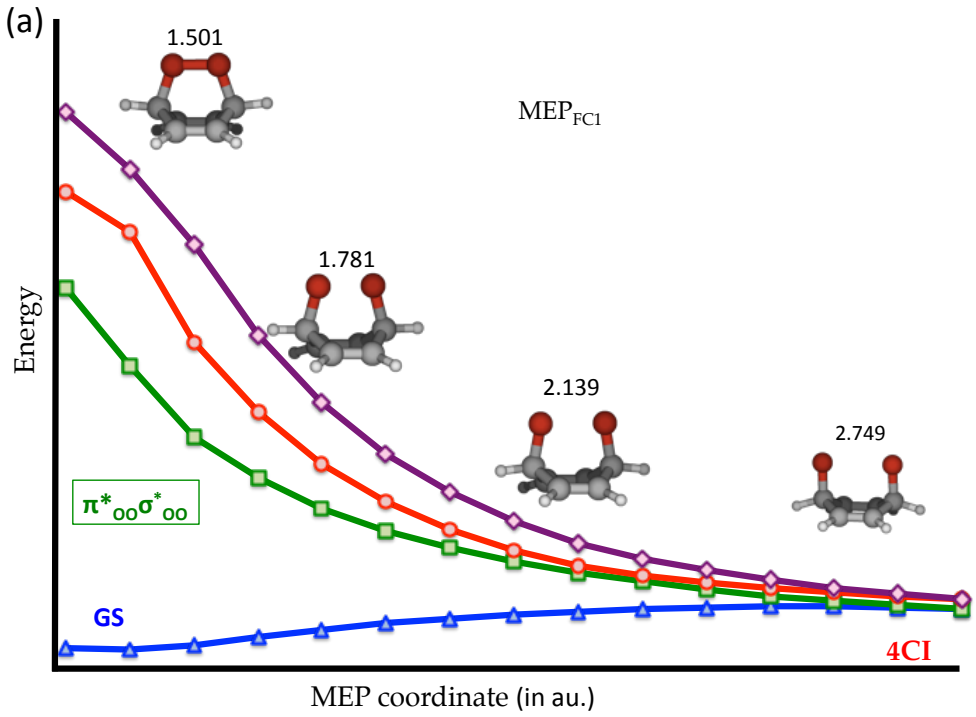

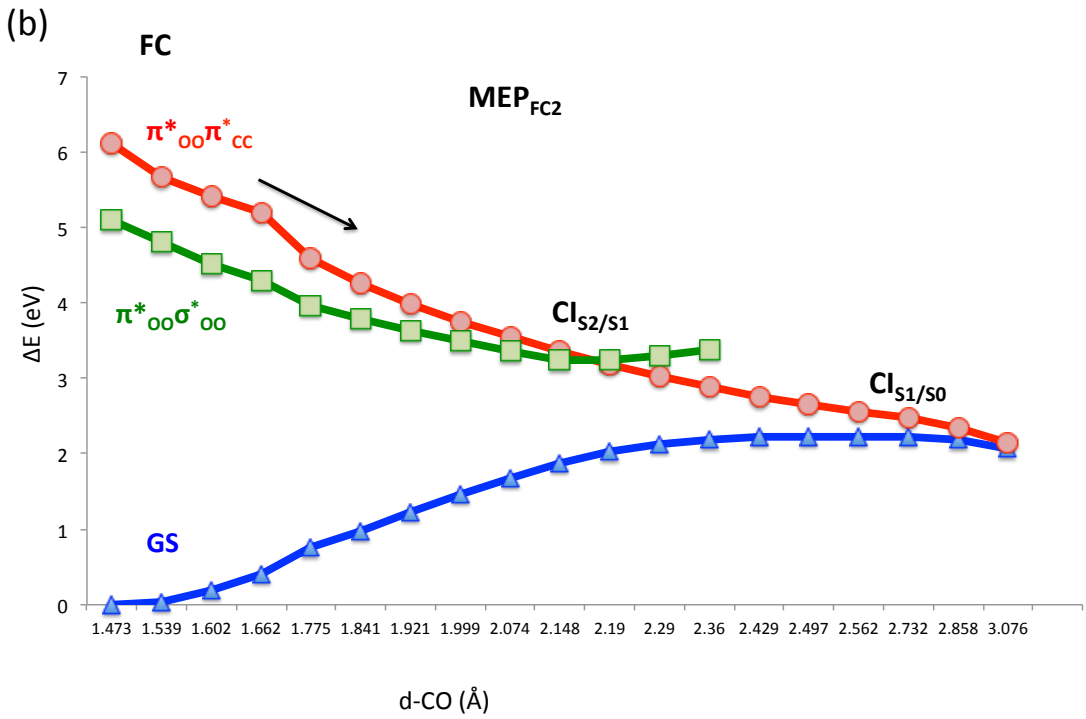

Figure S6. Simulated absorption spectra for CHDEPO. Black solid line depicts to the spectrum calculated using SA4-CASSCF(14,12)/ANO-RCC level of theory, and dotted contours represent the contribution of the different states to the absorption bands.

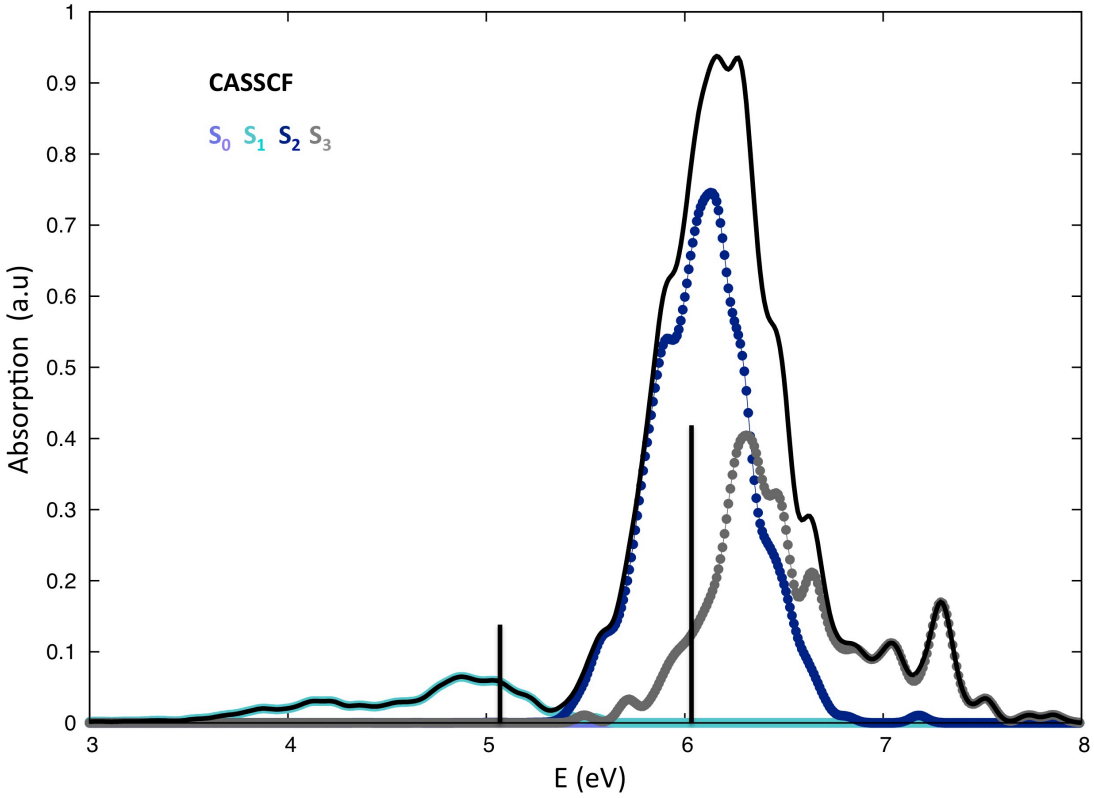

Figure S7. Simulated absorption spectra for CHDEPO. Red solid line represent the results obtained by performing further MS-CASPT2/ SA4-CASSCF(14,12)/ANO-RCC calculations., and dotted contours represent the contribution of the different states to the absorption bands.

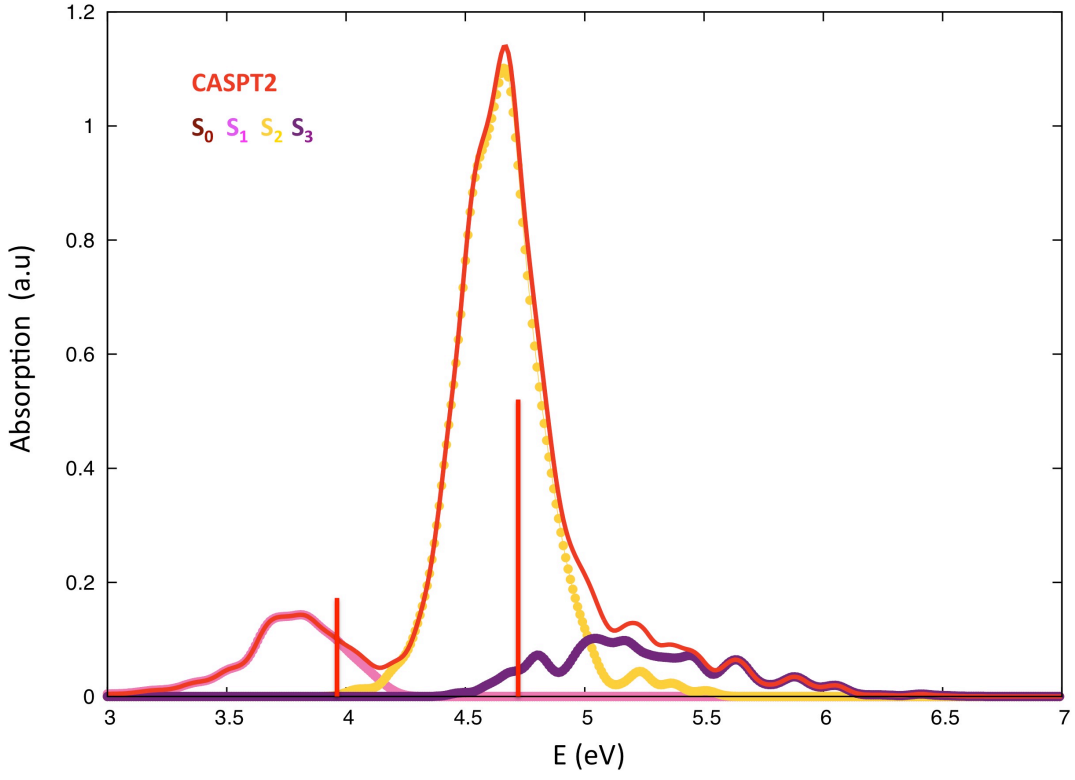

Figure S8. Time evolution of a representative trajectory resulting BQ and H_2 products. No labeling of the states is included since they correspond to spin-orbit states (presented in solid lines). The total energy in black points indicates the current state at each time.